Creation Research Society Quarterly 2021 58:76–84

Classification of the Enigmatic Red Panda *(Ailurus fulgens)* Based on Molecular Baraminology-Based Analysis

Matthew Cserhati*

Abstract

The red panda is a curiosity of biological classification. Taxonomists have come to different conclusions on its placement depending on which characteristics are considered. It was once considered closely related to bears (ursids), other times to raccoons (procyonids), or animals such as skunks (mephitids), badgers, otters, or martens (mustelids). Perhaps the red panda belongs to its own group.

Since the whole genome sequence was available for this organism, the Whole Genome k-mer Signature algorithm was used to classify the red panda. Mitochondrial DNA and cytochrome-b protein sequence similarity was also measured to help determine the baraminic status of the red panda.

According to the whole genome analysis, the red panda groups with the mustelids, apart from ursids. The placement of mephitids is uncertain. According to the mitochondrial DNA analysis, the red panda is part of a cluster discontinuous with mustelids and all other groups. However, when the sequence identity of the cytochrome-b protein is assessed, it appears that the red panda again shows continuity with mustelids, and discontinuity with ursids. Mephitids also show discontinuity with mustelids. The difference between the whole genome and mitochondrial results could be due to nucleo-mitochondrial discordance, a common phenomenon. A higher number of four-fold degenerate sites in the mitochondrial cyt-b compared to the first exon of the nuclear RAG1 gene support this.

Based on these results, it is likely that the red panda belongs to the mustelid holobaramin, although further baraminology studies are warranted, both morphological and molecular.

Key Words: Red panda, whole genome, mitochondrion, mephitid, mustelid, ursid

* Matthew Cserhati

Accepted for publication August 10, 2021

Introduction

Genesis 1:20–25 describes how God created fish, birds, and land-animals each according to their kinds. Species within a kind were originally capable of breeding with one another but are incapable of breeding with species from another kind. Hence, there is continuity between species within a kind, and discontinuity between two separate kinds. In technical terms, a kind is called a 'baramin,' which is a compound of two Hebrew words, 'bara' meaning 'he created,' and 'min' meaning kind. Thus, molecular baraminology is the study of the created kinds from a molecular biology perspective. A 'holobaramin' denotes all species which constitute a single baramin. A 'monobaramin' denotes either part of, or the entire holobaramin. This means it can also denote a specific lineage or subgroup within a holobaramin. For example, domesticated cats are a monobaramin within the cat holobaramin.

Most baraminology studies classify an entire set of species. However, there are many individual species that defy classification. These organisms do not resemble any other known organism, and as such are enigmatic. Such organisms include the duck-billed platypus, the tuatara (Cserhati, 2021a), and the echidna. These organisms could either belong to their own holobaramin, with all other related species within its group dying out, or they could possibly be related to other contemporary species, albeit in an unapparent way. Or it may even be that a holobaramin consists of but a single species, for example the human holobaramin, since only man was made in the image of God (Genesis 1:26–27). God probably created holobaramins with only one single species, but some kinds diversified more than others over time.

Looks can deceive, the saying goes, so alongside morphological analysis, a molecular baraminology analysis may unveil true baraminic relationships — another advantage of molecular methods augmenting with morphological ones. Whereas morphology studies may not detect variation within a species, the genome is more static, and thus its analysis may uncover the presence of more cryptically related species.

Figure 1. The red panda (*Ailurus fulgens*, upper left), the giant panda (*Ailuropoda melanoleuca*, lower left) raccoon (*Procyon lotor*, upper right), American marten (*Martes americana*, lower right). Copyright of images: red panda: en.wikipedia.org/wiki/Red_panda, giant panda: en.wikipedia.org/wiki/Giant_panda, raccoon: en.wikipedia.org/wiki/Raccoon, American marten: inaturalist.org/guide_taxa/335813.

One such hard-to-classify animal is the red panda (*Ailurus fulgens*). Distinguished by its bushy tail and red-white coloration, it is found in parts of Nepal, India, and China (Figure 1, upper left). Whereas *A. fulgens* denotes the Himalayan red panda, another subspecies exists, called the Chinese red panda (*Ailurus fulgens styani*). The two subspecies have been differentiated based on geographic isolation and genomic differences (Hu et al., 2020). According to Su et al. (2001) the genetic diversity of the mtDNA of the red panda shows that there are two major populations of the red panda in the provinces of Sichuan and Yunnan in China.

Theories about the exact position of the red panda abound. Geoffroy-Saint-Hilare and Cuvier originally classified the red panda as a member of the raccoon family (Procyonidae), although they ended up calling it *Ailurus*, because of its somewhat feline appearance (though this is subjective) (Slattery and O'Brien, 1995; Flynn et al., 2000). Some think that the red panda is related to the giant panda (*Ailuropoda melanoleuca*), because of its sesamoid bone, an enlarged toe-like structure, produced by an enlarged carpal bone (Hennigan, 2009; Abella et al., 2015). This modified bone is used to process bamboo, which makes up 99% of their diets. Still others place the red panda into its own family (Ailuridae) (Ledje and Arnason, 1999). More recent molecular-based studies of the red panda are somewhat divided, with some associating it with mustelids, procyonids, and mephitids (Fulton, 2007; Sato, 2009). Dragoo and Honeycutt (1997)

place *A. fulgens* within Procyonidae based on total evidence from the 12S, 16S rRNA and cytochrome-b genes, combined with morphological data.

Biblical considerations

The red panda is not mentioned anywhere in the Bible, so we must classify it based on genetic and genomic data.

Previous baraminology studies

Previous baraminology studies have not addressed the baraminic statues of the red panda in much depth. Hennigan (2010), for example, does not classify the red panda as a member of the bear holobaramin, despite mentioning several shared features with the giant panda (*A. melanoleuca*). Both types of pandas have a diet consisting almost exclusively of bamboo (both species eat meat on occasion), and an enlarged radial sesamoid bone, which they use to process bamboo. Genetic evidence classifies *A. melanoleuca* as a member of the family Ursidae. This includes analysis of the mtDNA analysis, chromosome banding patterns, and serological and immunological evidence (Yu et al., 2007; Krause et al., 2008).

Thompson and Wood studied craniodental characteristics of 'Cenozoic' mammal baramins but did not find any continuity or discontinuity between *A. fulgens* and Procyonidae (Thompson and Wood, 2018). *A. fulgens* also has some unique characteristics: a large zygomatic arch, a powerful jaw, and complex cheek teeth, following a P2–3 pattern, uncommon in carnivores. These evidences would support placing the red panda into its own group.

Materials and Methods

Sequence data

The whole genome sequences of 28 mammals were downloaded from NCBI, including organisms that are classified near *A. fulgens*, namely, species from the families Ursidae (bears), Procyonidae (raccoons), Mephitidae (skunks and stink badgers), Mustelidae (weasels, badgers, otters, ferrets, minks, martens, wolverines, etc.), and Felidae (cats). A list of these species and the link to their WGS can be found in Supplementary file 1 online. The WGS were analyzed using the Whole Genome K-mer Signature (WGKS) algorithm (Cserhati, 2020).

The mtDNA sequences of 52 mammals from these families were also downloaded from NCBI for analysis. The species and the accession number of their mtDNA sequences can be found online in Supplementary file 2.

A study focused on the sequence identity of the cytochrome-b protein sequence was also done for 51 species. These results are in Supplementary file 3. The cytochrome-b sequences were all downloaded from the NCBI Nucleotide database for these species. The mtDNA and cytochrome-b sequences were analyzed by looking at their sequence similarity.

To examine mito-nuclear discordance, both a mitochondrial gene and a nuclear gene of approximately the same length from *A. fulgens* and the closely related *A. fulgens styani* were aligned and examined for four-fold degeneracy in the third position of triplets in the mRNA sequence. These two genes were cytochrome-b (1,130 bp) and the first exon of RAG1 (1,095 bp). They can be seen in Table 4.

Software

Supplementary files 1, 2, and 3, and supplementary Figures 1 and 2 are available online at github.com/csmatyi/redpanda. The *Kalign* multiple alignment program was used with default parameters to create a multiple alignment of mtDNA sequences on the EBI website at ebi.ac.uk/Tools/msa/kalign (Lassmann, 2006). The alignment of the 51 cytochrome-b sequences were done using the *MUSCLE* algorithm (Edgar, 2004) using the MEGA-X software (Kumar et al., 2018). Using this software, the distance matrix was transformed into a similarity matrix by subtracting the distance values from 1. Heatmaps were created using the heatmap command in R, version 3.6.0. The 'ward.D', 'single', and 'mcquitty' algorithms were used to cluster organisms in the heatmaps for the WGKS, mtDNA and cyt-b analyses, respectively.

Results

Whole Genome K-mer Signature analysis

According to the protocol of the WGKS algorithm, the octamer signature for the WGS of 28 mammals was calculated and compared to one another to generate Pearson Correlation Coefficient (PCC) values. This PCC matrix was then visualized in a heatmap, in Figure 2. The Hopkins clustering statistic is 0.9, which denotes excellent clustering.

In Figure 2 we can see three groups, with the western spotted skunk (*Spilogala gracilis*) possibly as a singleton species in its own group. A silhouette plot was constructed for either three or four clusters. The average silhouette width is 0.82 in the case of three clusters (Supplementary Figure 1) and 0.8 for four clusters (Supplementary Figure 2). The difference is very slight. Based on this result, three putative baramins can be defined: felids covering the family Felidae (eleven species), ursids covering the family Ursidae (five species), and musteloids, a superfamily including Mephitidae and Mustelidae (twelve species). All three of these groups show statistically significant continuity within themselves and discontinuity with all other species in this study. Table 1 lists the results of the WGKS clustering, showing the species according to the cluster to which they belong.

A. fulgens has a mean PCC value of 0.877±0.011 (mean ± standard error of the mean, SEM) with all other members

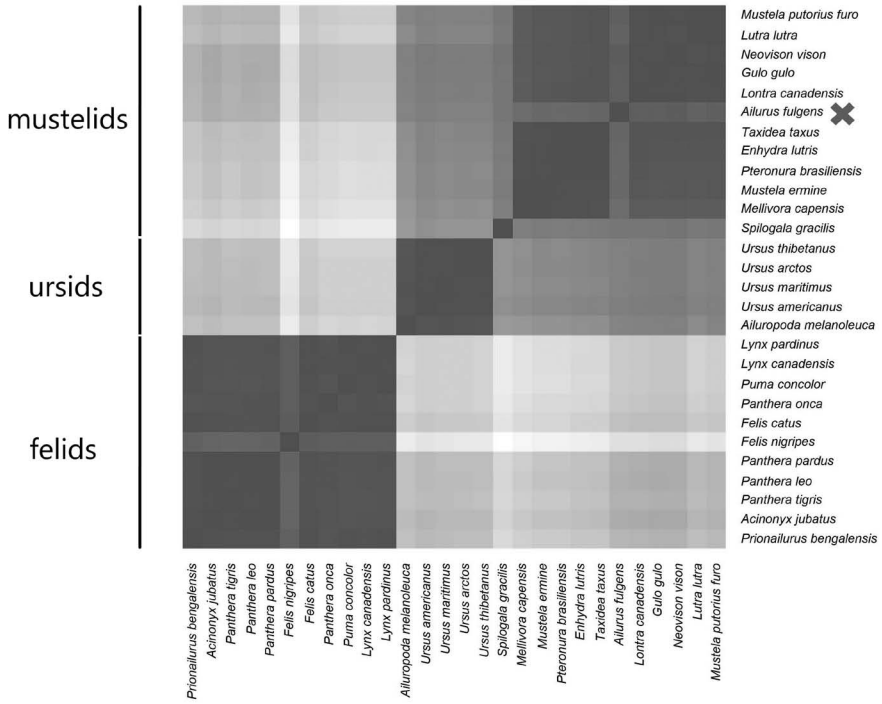

Figure 2. Heatmap showing baraminic relationships between *A. fulgens* (indicated by an X) and several ursid, mustelid, mephitid, and felid species. Each pixel in the heatmap represents the PCC value between the WGKS of two given species in the study. Species with high continuity have a high PCC value, which corresponds to darker colors. Species with high discontinuity have lower PCC values, represented by a lighter pixel. *A. fulgens* clusters nicely within Musteloidea, apart from felids and ursids, although with a lesser than average PCC value.

of the Musteloidea baramin. However, all other mustelids have a mean PCC value of 0.93±0.024, which is somewhat higher. The reason for the low mean PCC value between *A. fulgens* and all other mustelids might be its geographic isolation in the mountainous areas of Nepal, India, and China. This could have allowed for greater genetic change to take place.

This difference in PCC values does not seem significant if we look at the fact that the black-footed cat (*Felis nigripes*) has a mean PCC value of 0.9±0.005 with all other felids, whereas all other felids have a mean PCC of 0.98±0.003 among themselves. The black-footed cat definitely belongs to the cat holobaramin. *F. nigripes* is also an isolated species, found in South Africa, Namibia, Botswana, and Zimbabwe. It has been listed as a vulnerable species on the IUCN Red List since 2002, and in vitro fertilization and cryopreservation efforts are being undertaken to help preserve this species (Herrick et al., 2010).

A. fulgens has a mean PCC value of 0.73±0.004 with the five members of the ursid holobaramin, suggesting it is unrelated to bears. It has a mean PCC value of only 0.58±0.01 with the members of the felid baramin, meaning that it is also neither a cat, nor a ‹bear-cat.›

Analysis of the alignment of mtDNA sequences

Besides WGS, the mtDNA sequences of 15 ursids, 30 mustelids, 3 mephitids, and 2 procyonids as well as the two subspecies of the red panda were available at NCBI. These 52 mtDNA sequences

Table 1. Classification of 28 mammalian species based on the WGKS method. Group 1 consists of Mustelidae+Mephitidae, plus the red panda; Group 2 is all the species from Ursidae, and in Group 3 are all the species from Felidae from this study.

Species	Group
Ailurus fulgens	1
Enhydra lutris	1
Gulo gulo	1
Lontra canadensis	1
Lutra lutra	1
Mellivora capensis	1
Mustela ermine	1
Mustela putorius furo	1
Neovison vison	1
Pteronura brasiliensis	1
Taxidea taxus	1
Ailuropoda melanoleuca	2
Ursus americanus	2
Ursus arctos	2
Ursus maritimus	2
Ursus thibetanus	2
Acinonyx jubatus	3
Felis catus	3
Felis nigripes	3
Lynx canadensis	3
Lynx pardinus	3
Panthera leo	3
Panthera onca	3
Panthera pardus	3
Panthera tigris	3
Prionailurus bengalensis	3
Puma concolor	3
Spilogala gracilis	3

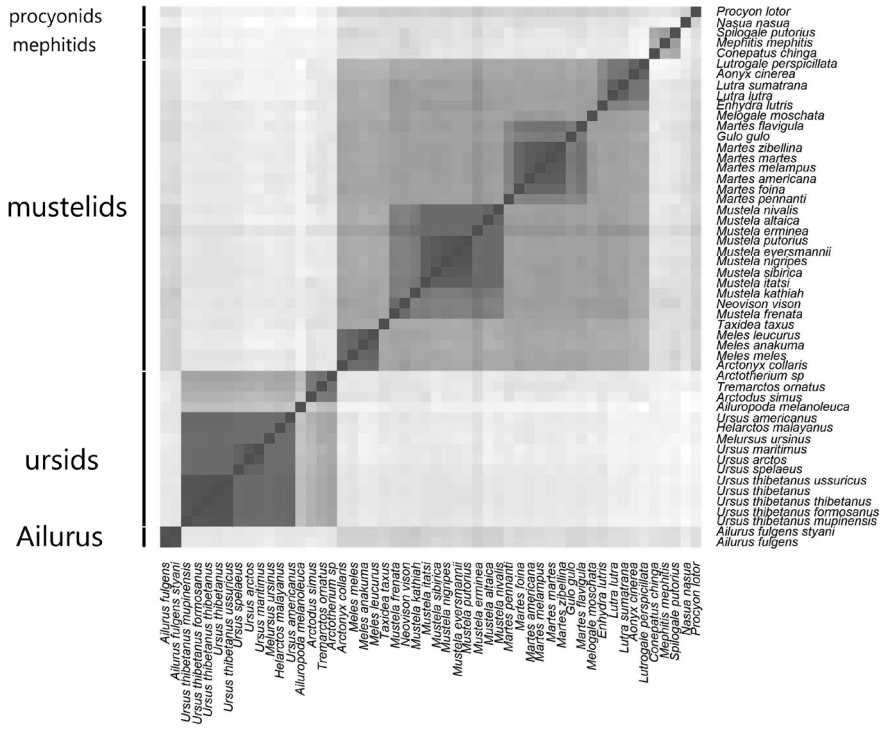

Figure 3. Heatmap showing baraminic relationships between two *Ailurus* species and several procyonid, mephitid, mustelid, and ursid species based on sequence similarity between their mtDNA sequences. Species with high continuity have a high PCC value, which corresponds to darker colors. Species with high discontinuity have lower PCC values, represented by a lighter pixel. The two *Ailurus* species and the three mephitids both form clusters separate from mustelids.

were aligned with the MUSCLE aligner software (Edgar, 2004). The resulting identity matrix showing global sequence similarity was visualized in a heat map (Figure 3). The list of species, their mtDNA accession numbers, the sequence identity matrix, the clusters and the baraminic classification statistics can be found in Supplementary file 2. The Hopkins clustering statistic is 0.841, which corresponds to good clustering. The list of species and their corresponding clusters can be seen in Table 2.

In this heatmap we can see two main, large clusters as well as three smaller ones. All five groups show statistically significant continuity among themselves and discontinuity with all other groups. Two small groups can be seen in the upper right, the first one being two procyonid species, *Procyon lotor* (the common raccoon), and *Nasua nasua* (the South American coati). Next are three mephitid species, *Spilogale putorius* (the eastern spotted skunk), *Mephitis mephitis* (the striped skunk), and *Conepatus chinga* (Molina's hog-nosed skunk). Thirty mustelid species make up the largest cluster, with species from the genera *Aonyx*, *Arctonyx*, *Enhydra*, *Gulo*, *Lutra*, *Lutrogale*, *Martes*, *Meles*, *Mustela*, *Neovision*, and *Taxidea*. Another large cluster with 15 ursid species can be seen to its lower left. This group is made up of the species *Arctodus simus*, *Arctotherium sp.*, *Ailuropoda melanoleuca*, *Helarctos malayanus*, *Melursus ursinus*, *Tremarctos ornatus*, and nine species of *Ursus*. In the lower left corner, we have the two red panda species, *A. fulgens*, and *A. fulgens styani*.

The findings of the mtDNA study contradict those of the whole genome analysis. It is true that the mtDNA is only a small fraction of the whole genome, so more weight should be given to the results of the WGKS analysis. However, some authors have found that *A. fulgens* is related to mustelid species. For example, Peng et al. (2017) placed *A. fulgens* next to *Martes americana*, the American marten in an analysis of 13 concatenated mtDNA proteins. Based on a study of the 12S rRNA, the 16S rRNA, and cytochrome-b, Flynn et al. (2000) also classified *A. fulgens* as a mustelid.

Protein sequence analysis of cytochrome-b

Cytochrome-b is a structurally conservative protein which does not mutate freely. It is often used to infer phylogenetic relationships between organisms (Meyer, 1994), and can so be used in baraminology studies as well. The cytochrome-b sequences of 51 felids, ursids, mustelids, procyonids and mephitids were aligned and the similarity matrix was determined using the MEGA-X software. The Hopkins clustering statistic is 0.8, which denotes good clustering. In Figure 4 we can see the heatmap which depicts the baraminic relationships between the 51 species. The species list, the identity matrix, the clusters, and the clustering statistics are available online in Supplementary file 3. The clustering results are available in Table 3.

In the heatmap (Figure 4) we can see three main clusters and two species by themselves, *N. nasua* and *M. mephitis*. In the lower left there is a tight cluster of 25 felids. In the upper right there is a cluster of five ursid species, and another with 19 mustelid species. All three larger clusters show statistically significant continuity among themselves and discontinuity with all other clusters.

Table 2. Classification of 52 mammalian species based on sequence identity calculated from the alignment of their mtDNA sequences. The numbers correspond to the following groups: 1: Ursidae, 2: Mephitidae, 3: Procyonidae, 4: Ailurus, 5: Mustelidae.

Species	Group	Species	Group
Ailuropoda melanoleuca	1	*Meles leucurus*	5
Melursus ursinus	1	*Melogale moschata*	5
Ursus spelaeus	1	*Martes pennanti*	5
Ursus arctos	1	*Gulo gulo*	5
Ursus maritimus	1	*Martes flavigula*	5
Helarctos malayanus	1	*Martes foina*	5
Ursus americanus	1	*Martes americana*	5
Ursus thibetanus mupinensis	1	*Martes melampus*	5
Ursus thibetanus formosanus	1	*Martes martes*	5
Ursus thibetanus thibetanus	1	*Martes zibellina*	5
Ursus thibetanus	1	*Mustela frenata*	5
Ursus thibetanus ussuricus	1	*Neovison vison*	5
Arctodus simus	1	*Mustela kathiah*	5
Tremarctos ornatus	1	*Mustela erminea*	5
Arctotherium sp.	1	*Mustela itatsi*	5
Conepatus chinga	2	*Mustela sibirica*	5
Mephitis mephitis	2	*Mustela nigripes*	5
Spilogale putorius	2	*Mustela eversmannii*	5
Nasua nasua	3	*Mustela putorius*	5
Procyon lotor	3	*Mustela nivalis*	5
Ailurus fulgens	4	*Mustela altaica*	5
Ailurus fulgens styani	4	*Enhydra lutris*	5
Taxidea taxus	5	*Lutra lutra*	5
Arctonyx collaris	5	*Lutra sumatrana*	5
Meles meles	5	*Aonyx cinerea*	5
Meles anakuma	5	*Lutrogale perspicillata*	5

The heatmap shows that *A. fulgens* and *A. fulgens styani* clustering together with mustelids. However, *M. mephitis* clusters away from the mustelids indicating that the skunk might possibly be from a separate holobaramin. This was also indicated in the WGKS analysis, where the average silhouette width was 0.8 for classifying *M. mephitis* by itself as opposed to the average silhouette width of 0.82 (a mere difference of 0.02) for putting them together with mustelids.

Degenerate sites between a nuclear and a mitochondrial gene in the two *A. fulgens* species

The accession number and the number of four-fold degenerate triplet third positions of the mitochondrial gene cytochrome-b and the first exon of the nuclear gene RAG1 between *A. fulgens* and *A. fulgens styani* are shown in Table 4. For the mitochondrial gene cytochrome-b there are nine degenerate positions, whereas for exon 1 of the nuclear gene RAG1, there are none. The mitochondrial gene has undergone more mutations, and thus is more degenerate. Therefore, it makes sense that its mtDNA sequence has also diverged more than the nuclear genome.

Other studies have found similar results. For example, Su et al. (2001) found 25 haplotypes in 17 polymorphic positions in an analysis of a 236-bp region of the D-loop region of the mtDNA in 53 red pandas. This is another indication that mtDNA mutates faster than nuclear DNA.

This can explain why the WGS, mtDNA, and cytochrome-b results are divergent. It also shows the importance of performing multiple analyses using different data sets on the same group of organisms. A faster mutation rate means larger differences in the mtDNA sequence in contrast with the nuclear genome. This may reveal lineages within a kind, which might appear to be separate baramins.

Discussion

Based on all this evidence, how do we then classify *A. fulgens*? Based on the somewhat differing results between the WGKS and the cytochrome-b analysis compared to the results of the mtDNA analysis, can we say anything definitive about which holobaramin *A. fulgens* belongs to?

The WGKS analysis seems to bring the strongest results, since it is a global analysis of the entire genome. Accord-

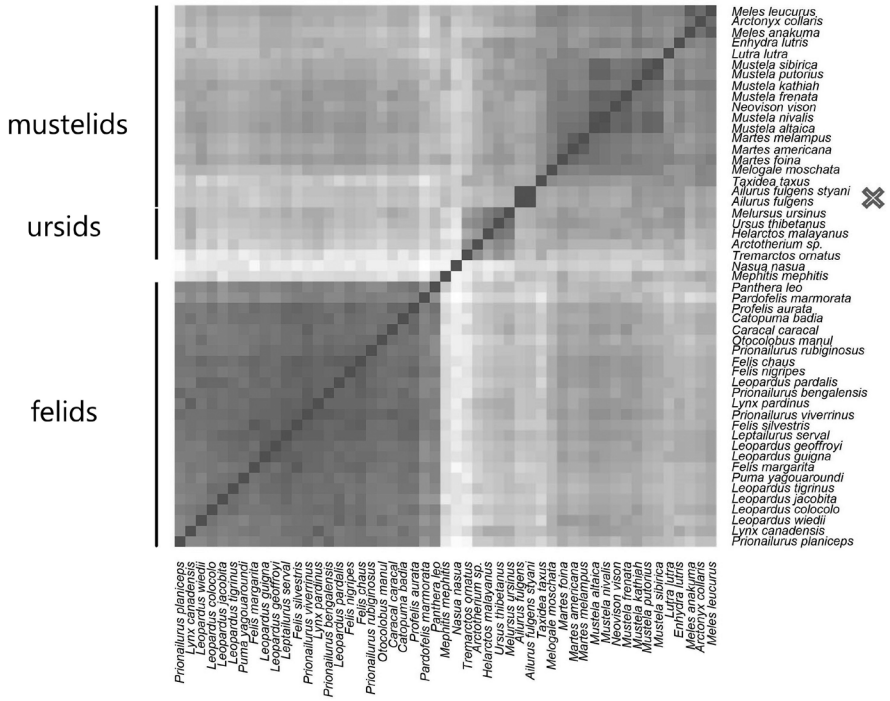

Figure 4. Heatmap showing baraminic relationships between two *Ailurus* species (indicated by the X) and several felid, ursid, mustelid, mephitid and procyonid species based on sequence similarity of the cytochrome-b protein. Species with high continuity have a high sequence similarity, which corresponds to darker colors. Species with low discontinuity have lower sequence similarity, represented by a lighter pixel. The two *Ailurus* species cluster with mustelids. *M. mephitis* does not cluster with mustelids+*Ailurus*

ing to this analysis, *A. fulgens* belongs to the mustelid holobaramin. Also, *M. mephitis* could either belong to the mustelid holobaramin, or it could either belong to another holobaramin, due to the minimal differences in average silhouette width values. Genomically, *A. fulgens* shares several apomorphic chromosome fusions with mustelids, namely F2+C1p and A1p+C1q (Nie, 2002). However, *A. fulgens* differs in several other chromosomal rearrangements indicating that it diverged early from the mustelids. In contrast, the mtDNA is only a small fraction of the entire genome and contains only a handful of genes. According to the mtDNA results, *A. fulgens* seems to cluster away from mustelids and to belong to its own group. Mephitids also form another cluster. But when we look at the heat map in Figure 4 on cytochrome-b sequence similarity it appears that *A. fulgens* clusters together with mustelids, with mephitids again forming their own holobaramin.

What could be causing the difference? A possibility could be something called mito-nuclear discordance, which entails differences between selective and mutational pressures between nuclear and mitochondrial DNA. This is a common phenomenon and can be caused by migration of organisms (Toews and Brelsford, 2012; Morales et al., 2015; Bernardo et al., 2019).

Alternatively, *A. fulgens* could be the only known member of its own holobaramin, as mentioned in the Introduction and supported by the mtDNA results. Such a phenomenon is not uncommon. When a taxon, as in this case, a holobaramin loses a large portion of its constituent species, during a mass extinction, such as the Genesis Flood, it loses its capability to re-diversify after the extinction. Such taxa include the bivalve genera *Permophorus* and *Linearia* (Jablonski, 2002), bellerophontid snails, prolecanitid ammonoids (Jablonski, 2001) the tuatara (*Sphenodon punctatus*) (Cserhati, 2021a), and parareptiles (MacDougall, 2019). Taxa that find physical refuge can also exist for long periods of time without going extinct. *A. fulgens* may be the sole survivor of its own holobaramin, living in geographic isolation in mountainous habitats of India, China, and Nepal.

Summary and Conclusion

Based on all of these considerations, it is likely that *A. fulgens* belongs to the mustelid holobaramin, and not the ursid holobaramin. Mephitids also very likely form a separate holobaramin apart from mustelids. This is a result similar to the one found by Cserhati (2021b) in a similar analysis.

Acknowledgements

This paper is a part of Creation Research Society Grant #62 and part of the analysis was performed on the new CRS server based at Arizona Christian University.

References

CRSQ: *Creation Research Society Quarterly*

Abella, J., A. Pérez-Ramos, A. Valenciano, D.M. Alba, M.D. Ercoli, D. Hontecillas, P. Montoya, and J. Morales. 2015. Tracing the origin of the panda's thumb. *Die Naturwissenschaften* 102(5–6):35.

Bernardo, P.H., S. Sánchez-Ramírez, S.J. Sánchez-Pacheco, S.T. Álvarez-Castañeda, E.F. Aguilera-Miller, F.R. Mendez-de la Cruz, and R.W. Murphy. 2019.

Table 3. Baraminic classification of 51 mammals based on their sequence identity of the cytochrome-b protein. The numbers correspond to the following groups: 1: Mustelidae+*Ailurus*, 2: Felidae, 3: Mephitidae, 4: Procyonidae, 5: Ursidae.

Species	Group	Species	Group
Ailurus fulgens	1	*Leopardus geoffroyi*	2
Ailurus fulgens styani	1	*Leopardus guigna*	2
Arctonyx collaris	1	*Leopardus jacobita*	2
Enhydra lutris	1	*Leopardus pardalis*	2
Lutra lutra	1	*Leopardus tigrinus*	2
Martes americana	1	*Leopardus wiedii*	2
Martes foina	1	*Leptailurus serval*	2
Martes melampus	1	*Lynx canadensis*	2
Meles anakuma	1	*Lynx pardinus*	2
Meles leucurus	1	*Otocolobus manul*	2
Melogale moschata	1	*Panthera leo*	2
Mustela altaica	1	*Pardofelis marmorata*	2
Mustela frenata	1	*Prionailurus bengalensis*	2
Mustela kathiah	1	*Prionailurus planiceps*	2
Mustela nivalis	1	*Prionailurus rubiginosus*	2
Mustela putorius	1	*Prionailurus viverrinus*	2
Mustela sibirica	1	*Profelis aurata*	2
Neovison vison	1	*Puma yagouaroundi*	2
Taxidea taxus	1	*Mephitis mephitis*	3
Caracal caracal	2	*Nasua nasua*	4
Catopuma badia	2	*Arctotherium sp.*	5
Felis chaus	2	*Helarctos malayanus*	5
Felis margarita	2	*Melursus ursinus*	5
Felis nigripes	2	*Tremarctos ornatus*	5
Felis silvestris	2	*Ursus thibetanus*	5
Leopardus colocolo	2		

Extreme mito-nuclear discordance in a peninsular lizard: The role of drift, selection, and climate. *Heredity* 123(3):359–370.

Cserhati, M. 2020. A new baraminology method based on Whole Genome K-mer Signature analysis and its application to insect classification. *Journal of Creation* 34(1):86–95.

Cserhati, M. 2021a. Baraminic classification of the tuatara (*Sphenodon punctatus*) among reptiles based on whole genome k-mer signature comparison. *CRSQ* 57(3):200–205.

Cserhati, M. 2021b. A tail of two pandas—Whole Genome K-mer Signature analysis of the red panda (*Ailurus fulgens*) and the giant panda (*Ailuropoda melanoleuca*). *BMC Genomics* 22(1):228.

Dragoo, J.W., and R.L. Honeycutt. 1997. Systematics of mustelid-like carnivores. *Journal of Mammology* 78(2):426–441.

Edgar, R.C. 2004. MUSCLE: Multiple sequence alignment with high accuracy and high throughput. *Nucleic Acids Research* 32(5):1792–1797.

Flynn, J.J., M.A. Nedbal, J.W. Dragoo, and R.L. Honeycutt. 2000. Whence the red panda? *Molecular Phylogenetics and Evolution* 17(2):190–99.

Fulton, T.L., and C. Strobeck. 2007. Novel phylogeny of the raccoon family (Procyonidae: Carnivora) based on nuclear and mitochondrial DNA evidence. *Molecular Phylogenetics and Evolution* 43(3):1171–1177.

Hennigan, T. 2010. The case for holobaraminic status in bears (family Ursidae) and the implications within

Table 4. *A. fulgens* genes and the number of four-fold degenerate sites at the third triplet position.

Species	Gene	Accession	Degenerate triplet positions
A. fulgens	Cytochrome-b (mitochondrion)	NC_011124.1:14171–15310	9
		AB291074.1:14173–15312	
A. fulgens styani	RAG1, exon 1 (nucleus)	AB188525.1	0
		AB302261.1	

a creation model of ecology. *CRSQ* 46(4):271–283.

Herrick, J.R., M. Campbell, G. Levens, T. Moore, K. Benson, J. D'Agostino, G. West, D.M. Okeson, R. Coke, S.C. Portacio, K. Leiske, C. Kreider, P.J. Polumbo, and W.F. Swanson. 2010. In vitro fertilization and sperm cryopreservation in the black-footed cat (*Felis nigripes*) and sand cat (*Felis margarita*). *Biology of Reproduction* 82(3):552–562.

Jablonski, D. 2001. Lessons from the past: Evolutionary impacts of mass extinctions. *Proceedings of the National Academy of Sciences of the USA* 98(10):5393–5398.

Jablonski, D. 2002. Survival without recovery after mass extinctions. *Proceedings of the National Academy of Sciences of the USA* 99(12):8139–8144.

Krause, J., T. Ungar, A. Noçon, A.S. Malaspinas, S.O. Kolokotronis, M. Stiller, L. Soibelzon, H. Spriggs, P.H. Dear, A.W. Briggs, S.C. Bray, S.J. O'Brien, G. Rabeder, P. Matheus, A. Cooper, M. Slatkin, S. Pääbo, and M. Hofreiter. 2008. Mitochondrial genomes reveal an explosive radiation of extinct and extant bears near the Miocene-Pliocene boundary. *BMC Evolutionary Biology* 8(220):1–12.

Kumar, S., G. Stecher, M. Li, C. Knyaz, and K. Tamura. 2018. MEGA X: Molecular Evolutionary Genetics Analysis across computing platforms. *Molecular Biology and Evolution* 35(6):1547–1549.

Lassmann, T., and E.L. Sonnhammer. 2006. Kalign, Kalignvu and Mumsa: Web servers for multiple sequence alignment. *Nucleic Acids Research* 34(Web Server issue):W596–599.

Ledje, C., and U. Arnason. 1999. Phylogenetic relationships within caniform carnivores based on analyses of the mitochondrial 12S rRNA gene. *Journal of Molecular Evolution* 43(6):641–649.

MacDougall, M.J., N. Brocklehurst, and J. Fröbisch. 2019. Species richness and disparity of parareptiles across the end-Permian mass extinction. *Proceedings of the Royal Society B:. Biological Sciences* 286(1899):20182572.

Meyer, A. 1994. Shortcomings of the cytochrome *b* gene as a molecular marker. *Trends in Ecology & Evolution* 9(8):278–280.

Morales, H.E., A. Pavlova, L. Joseph L, and P. Sunnucks. 2015. Positive and purifying selection in mitochondrial genomes of a bird with mitonuclear discordance. *Molecular Ecology* 24(11):2820–2837.

Nie, W., J. Wang, P.C. O'Brien, B. Fu, T. Ying, M.A. Ferguson-Smith, and F. Yang. 2002. The genome phylogeny of domestic cat, red panda and five mustelid species revealed by comparative chromosome painting and G-banding. *Chromosome Research* 10(3):209–222.

Peng, R., B. Zeng, X. Meng, B. Yue, Z. Zhang, and F. Zou. 2017. The complete mitochondrial genome and phylogenetic analysis of the giant panda (*Ailuropoda melanoleuca*). *Gene* 397(1–2):76–83.

Sato, J.J., M. Wolsan, S. Minami, T. Hosoda, M.H. Sinaga, K. Hiyama, Y. Yamaguchi, and H. Suzuki. 2009. Deciphering and dating the red panda's ancestry and early adaptive radiation of Musteloidea. *Molecular Phylogenetics and Evolution* 53(3):907–922.

Slattery, J.P., and S.J. O'Brien. 1995. Molecular phylogeny of the red panda (*Ailurus fulgens*). *The Journal of Heredity* 86(6):413–422.

Su, B., Y. Fu, Y. Wang, L. Jin, and R. Chakraborty. 2001. Genetic diversity and population history of the red panda (*Ailurus fulgens*) as inferred from mitochondrial DNA sequence variations. *Molecular Biology and Evolution* 18(6):1070–1076.

Thompson, C., and T.C. Wood. 2018. A survey of Cenozoic mammal baramins. In *Proceedings of the Eighth International Conference on Creationism*, J.H. Whitmore (editor), pp. 217–221, A1-A83 (appendix). Creation Science Fellowship, Pittsburgh, PA.

Toews, D.P., and A. Brelsford. 2012. The biogeography of mitochondrial and nuclear discordance in animals. *Molecular Ecology* 21(16):3907–3930.

Yu, L., Y.W. Li, O.A. Ryder, and Y.P. Zhang. 2007. Analysis of complete mitochondrial genome sequences increases phylogenetic resolution of bears (Ursidae), a mammalian family that experienced rapid speciation. *BMC Evolutionary Biology* 7:198.